

University of New Hampshire
University of New Hampshire Scholars' Repository

Honors Theses and Capstones

Student Scholarship

Spring 2012

Phosphate Availability During Sediment Resuspension Events in the Great Bay Estuary

Taylor Langkau

University of New Hampshire - Main Campus

Follow this and additional works at: <https://scholars.unh.edu/honors>



Part of the [Biogeochemistry Commons](#), and the [Sedimentology Commons](#)

Recommended Citation

Langkau, Taylor, "Phosphate Availability During Sediment Resuspension Events in the Great Bay Estuary" (2012). *Honors Theses and Capstones*. 56.

<https://scholars.unh.edu/honors/56>

This Senior Honors Thesis is brought to you for free and open access by the Student Scholarship at University of New Hampshire Scholars' Repository. It has been accepted for inclusion in Honors Theses and Capstones by an authorized administrator of University of New Hampshire Scholars' Repository. For more information, please contact nicole.hentz@unh.edu.

Phosphate Availability during Sediment Resuspension Events in the Great Bay Estuary

Taylor Langkau

UNH Department of Earth Sciences
ESCI799 Senior Thesis
Advisor: Linda Kalnejais

Abstract

Phosphorus is a very important nutrient in marine ecosystems, but it tends to adsorb to marine sediments, limiting its bioavailability. The mechanisms of phosphate adsorption to marine sediments are poorly understood and have not been well-quantified. In this experiment, Great Bay Estuary sediments were collected to compare phosphate adsorption characteristics in bulk sediment versus resuspended sediment in a simulated erosion experiment. Resuspended sediment was collected at increasing shear stresses, and phosphate adsorption experiments were conducted and analyzed using the phosphomolybdenum blue method (Strickland & Parsons, 1977). One sample was conducted in an oxygen free environment to examine the effects of redox chemistry on adsorption characteristics.

Results showed that resuspended sediment had higher adsorption capacities than bulk sediment, and the ability to adsorb phosphate increased with increasing shear stress. An anoxic environment limited the phosphate adsorption capacity. This is due to the inhibited formation of iron oxides, which bind phosphate very strongly. Future research could examine the mineralogy of the sediments including phosphorus phases and iron content. This experiment was conducted in the winter when phosphorus is depleted, so additional work investigating the change in adsorption characteristics with the seasons should also be undertaken.

Introduction

The Great Bay Estuary of the New Hampshire seacoast region has experienced significant environmental degradation and decreases in water quality over the past forty years. According to the State of the Estuaries report in 2009, the most pressing problems involve local population growth and the associated changes in nutrient loads and non-point source pollution. Population growth in the Great Bay area has caused an increase in nutrient load to the Great Bay and its tributaries. From 2004 – 2009, the nitrogen load to Great Bay increased by 42% (PREP, 2009). Nutrients play an active role in important biological processes such as primary production and decomposition.

Some nutrients in the water are beneficial to biological systems, but excessive concentrations can become hazardous. High nutrient concentrations in water can cause harmful algal blooms and changes in species composition (PREP, 2009). Algal decomposition may deplete dissolved oxygen in waters due to oxygen demand for decomposition of organic matter. Dissolved oxygen is an important component of water quality, and some sampling sites of the Great Bay Estuary have not met state-mandated water quality standards. The average concentrations of suspended solids and chlorophyll-a from the periods 1974-1981 to 2001-2008 have also increased dramatically. These parameters are an indicator of primary production occurring in the estuary. Suspended solids increased by 123% and chlorophyll-a by 28% during the approximately thirty year time period (PREP, 2009).

Increases in development due to population growth have also affected the percentage of impervious surfaces built on land surrounding the estuary. Impervious surfaces pose a hazard to water quality due to the fluid transport of pollutants such as hazardous chemicals, nutrients, and sediment that settle on them. Because water is not able to infiltrate the surface, storm water and other forms of precipitation transport these materials into the local waterways. The Piscataqua

Region Estuaries Partnership (PREP, 2009) cites that development creates new impervious surfaces at a current rate of 1,500 acres per year in the Piscataqua Region surrounding the Great Bay Estuary. In 2005, this represented an average of 7.5% of the watershed (PREP, 2009).

To further understand the implications of population growth on the dynamics of estuarine systems such as the Great Bay, it is beneficial to understand the effects of increased nutrient load in these water bodies. The major nutrient inputs to estuaries include terrestrial, atmospheric, industrial, point, and non-point sources (Warnken et al., 2000). Estuaries and other coastal regions receive more nutrients than open ocean waters due to the input from inland freshwater sources. Rivers and streams carry substances such as fertilizers and human and animal waste that are major sources of nutrients and pollutants. Eutrophication becomes an issue in many coastal waters. Eutrophication is the addition of nutrients in excess of what is needed for a normally functioning ecosystem. Estuaries are more prone to eutrophication than open ocean waters not just because they get more nutrients but also because they often have long residence times. The ocean is much better flushed than estuaries, so there is less time for phytoplankton to grow. Algal blooms may result, which may cause oxygen depletion (hypoxia) and fish kills if they persist for long periods of time.

One extreme example of the effects of eutrophication is the well-known “dead zone” where the Mississippi River enters the Gulf of Mexico. The Mississippi Drains 31 states and 40% of US agriculture, and it carries a nutrient load of 1.6 million tons of nitrogen and 100,000 tons of phosphorus annually (Joyce, 2000). This addition of anthropogenic nutrients into the Gulf of Mexico causes extensive algal blooms and hypoxic to anoxic conditions that extend from Louisiana to Texas and cover an area ranging from 5,000 to over 15,000 square kilometers (Diaz & Rosenberg, 2008). This is the second largest dead zone in the world, and it is a real-life

example of the effects of anthropogenic nutrient inputs to once thriving ecosystems. The Great Bay has much smaller nutrient fluxes (approximately 1,558 tons nitrogen per year from 2006 – 2008), so observed changes are much less prominent (PREP, 2009). However, the Great Bay is also a much smaller environment than the Gulf of Mexico is.

After reviewing nutrient inputs to a coastal ecosystem, it is important to understand the factors that control the storage, release, and use of the nutrients once they reach bodies of water such as an estuary. According to Zhang et al. (2004), over 90% of the total phosphorus that is transported into estuarine and coastal regions comes from river born suspended particulate matter. Most of that particulate matter settles out into the bottom sediments (Zhang et al., 2004). This creates a significant reservoir of phosphorus in the sediments and also in suspended matter in the water column (Zhang et al., 2004).

Sediment mineral composition plays a role in storage and release of nutrients. Phosphate can be strongly adsorbed to sediments, especially if the surface layers are oxygenated (Warnken et al., 2000). Adsorption is the chemical binding of a material to a surface. In sediments, the available adsorption surfaces come from the many different constituents of the sediments including organic matter, iron oxides, and clay particles. Different minerals found in the sediments have different adsorption capacities for nutrients such as phosphate. “Amorphous iron oxides have been shown to have the greatest adsorption capacity for phosphate” (Zhang & Huang, 2007, p. 2789). Phosphate also adsorbs to calcite and aragonite (Zhang et al., 2004). In general, dissolved phosphate, or PO_4^{3-} , has a strong affinity to solid surfaces, which makes it less bio-available as a macronutrient (Zhang & Huang, 2007).

Phosphate uptake is characterized by a two-step process. The first step is an initial “chemisorption”, which is very fast (Zhang et al., 2004). The second step is a slow solid-state

diffusion of adsorbed phosphate into the interior of the particles (Zhang et al., 2004; Froelich, 1988). Processes such as adsorption-desorption and coprecipitation-dissolution are major sources of dissolved phosphate in water, especially when these reactions occur at the sediment-water interface (Zhang & Huang, 2007). Gaining a better understanding of phosphorus bioavailability will aid in a better understanding of biomass and production of aquatic ecosystems such as the Great Bay Estuary.

Nutrient release from sediments occurs through both physical and biological processes. Physical processes include sediment resuspension due to winds and tides (Warnken et al., 2000). Finer particles are easier to resuspend in the water column by tidal or wind mixing, and they also have a longer residence time than larger particles (Zhang et al., 2004). Fine sediment particles make up a small proportion of sediment weight but a large proportion of total surface area, maximizing the space for phosphate adsorption (Zhang et al., 2004). Therefore, the amount of phosphorus that can be supplied to the water via sediment resuspension depends on the quality and size of resuspended particles and on the abundance of dissolved phosphorus in near-surface sediments (Zhang et al., 2004).

Organic matter found in sediments is also a potential source of nutrients. When microbial organisms in the sediments decompose organic matter, they release nutrients into sedimentary pore fluids, usually as nitrate or ammonium and phosphate. These dissolved nutrients can be introduced into the water column, the rate depending on environmental conditions such as oxygen availability and temperature (Lyons, 1982). Nutrient concentrations in porewater can be much higher than in the rest of the water column (Warnken et al., 2000). In the Great Bay Estuary, nutrient dynamics in the top 8-20 cm of sediment are largely controlled

by microfaunal activity (Lyons, 1982). Some marine organisms such as benthic algae and phytobenthos reduce the availability of porewater nutrients for exchange (Lyons, 1982).

Phosphorus behavior in sediments is not well understood due to the difficulty of distinguishing between the inert and bio-reactive forms of phosphate (Froelich, 1988). Some things about phosphorus are known although much still needs to be researched. It has one stable isotope, exists in one oxidation state, and has no significant fluxes besides river input from eroded continental rocks (Froelich, 1988). Phosphorus is found in over 250 minerals on Earth (Froelich, 1988). In order to better understand phosphorus dynamics in the ocean, the geochemistry of phosphorus and mineralogy of marine sediments need to be explored in further depth.

The goal of this project was to characterize the strength of phosphate binding in surface sediments in Great Bay and then compare this binding capacity to the binding capacity of resuspended sediments. The binding capacity as a storm progresses was simulated using an erosion chamber along with the effect of redox chemistry, which was performed using experiments with anoxic conditions.

Methods

Bulk Sediment Sampling

Bulk sediments were sampled in order to compare adsorption characteristics to eroded particles from the same location. Samples were taken at the UNH Jackson Estuarine Laboratory mud flats during low tide on February 28, 2012. Conditions during sampling were sunny, partly cloudy, and about 32°F. Syringe samplers were used to collect six sediment samples to a depth of about 5 cm. Three samples were used for porewater extraction and porewater phosphate

determination. The top 1 cm of the three remaining sediment samples were used for phosphate adsorption experiments.

Simulation of Sediment Erosion

A sediment core was collected from the UNH Jackson Estuarine Laboratory mud flats during low tide on March 12, 2012, and weather conditions were sunny, clear, and approximately 65°F. An erosion chamber (Kalnejais et al., 2007) was used to apply increasing shear stresses on the sediment ranging from 0.0 to 0.44 N/m². Samples of the suspended material were collected at three chosen shear stress steps. The shear stresses chosen were 0.33, 0.39, and 0.44 N/m². The suspended sediment sample from a shear stress of 0.44 N/m² was divided, and half of the sample was maintained under nitrogen gas to exclude the effects of oxygen. A known volume of seawater containing the suspended sediment at each of eight shear stresses was collected and filtered on pre-weighed filter paper. The mass of the filtered suspended solids was used to determine total suspended solids (TSS). Depth eroded into the sediment at each shear stress was calculated using water volume in the chamber, core barrel diameter, sediment porosity, density of solids in the sediment, and TSS. To obtain sediments for the phosphate adsorption experiments, the suspended material in the three seawater collections was allowed to settle for 24 hours before decanting water and collecting sediment.

Determination of the Phosphate Adsorption Characteristics

Sediment from the bulk sample and the erosion experiment, excluding the one sample under nitrogen gas, was dried at 60 °C to constant weight. The procedure of Zhang and Huang (2007) was followed to determine the adsorption characteristics of the sediments; this method is

described below. For each experiment, 50 mg of dried sediment was mixed with 25 mL of seawater collected at the Jackson Estuarine Lab. The natural phosphate concentration in the seawater was previously determined using the phosphomolybdenum blue method (Strickland & Parsons, 1977). Phosphate solutions made from KH_2PO_4 was added to each seawater sample to make known concentrations of 0, 10, 20, 30, 40, and 50 μM . Each of these six concentrations was used in bulk sediment and erosion sediment phosphate adsorption experiments. Samples were shaken on a benchtop shaker for 24 hours and then filtered with a 0.45 μm syringe filter. Seawater phosphate concentrations were analyzed using the phosphomolybdenum blue method (Strickland & Parsons, 1977). The equilibrium phosphate concentration (the final phosphate concentration P_f or EPC) and the amount of phosphate taken up by the sediments ($\Delta[\text{P}_{\text{sed}}] = P_i - P_f$) were determined.

Sample under Nitrogen Methods

One sample from the erosion experiment with a shear stress of 0.44 N/m^2 was investigated under an oxygen-free atmosphere. The TSS sample was removed from the erosion chamber, split as described earlier, and transferred to a glove bag filled with nitrogen gas. The sample was transferred to the glove bag two hours after collection. The seawater containing the suspended material was gravity filtered, and the sediments were dried to constant weight in the glove bag. Once dry, the procedure above for phosphate adsorption was followed entirely in the glove bag. Adsorption data was compared to erosion experiment data that was not conducted under nitrogen gas.

Calculations

A plot of $\Delta[P_{\text{sed}}]$ versus EPC was made for each sample. The data were linearized using a log plot of the equation that assumes phosphate adsorption follows Freundlich adsorption behavior:

$$\Delta[P_{\text{sed}}] + \text{NAP} = K_f([P]_f)^n \quad (\text{Equation 1}) \text{ (Zhang \& Huang, 2007).}$$

In the equation above,

$$\Delta[P_{\text{sed}}] = [P]_i - [P]_f \quad (\text{Equation 2}) \text{ (Zhang \& Huang, 2007),}$$

NAP is the native adsorbed phosphate, n is the exponential factor, and K_f is the Freundlich coefficient (Zhang & Huang, 1977). NAP was calculated by finding the y-intercept of a linear fit of the EPC vs. $\Delta[P_{\text{sed}}]$ plot. Using a log plot of equation 1:

$$\log_{10}(\Delta[P_{\text{sed}}] + \text{NAP}) = n \times \log_{10}([P]_f) + \log_{10}(K_f) \quad (\text{Equation 3})$$

n was calculated by finding the slope of the linearized data. K_f , the Freundlich coefficient, was determined from the y-intercept of the linearized data plot. Finally, K_d , which is the linear adsorption coefficient was determined using the equation:

$$K_d = n \times K_f \times ([P]_f)^{n-1} \quad (\text{Equation 4}) \text{ (Zhang \& Huang, 1977).}$$

K_d is defined as “the number of mol of phosphate adsorbed to (or desorbed from) the sediments required to change the phosphate concentration in water by 1 mol/L near the EPC_0 ” (Zhang & Huang, 2007, p. 2790). The EPC_0 is the zero equilibrium phosphate concentration, which is the concentration at which there is equilibrium in terms of phosphate exchange at the sediment-water interface (Zhang & Huang, 2007).

Results and Discussion

Bulk Sediment

Bulk Sediment Core	0 – 1 cm Porewater [PO ₄ ³⁻] (μM)	2 – 3 cm Porewater [PO ₄ ³⁻] (μM)	Bottom Porewater [PO ₄ ³⁻] (μM)
4	10.5	15.5	14.8
5	22.0	29.6	32.4
6	18.5	13.4	11.3

Table 1: Porewater concentrations for the three bulk sediment cores sampled. Bottom porewater was extracted from 2-3 cm depth for cores 5 and 6 and 2-5 cm depth for core 4.

The average surface porewater concentration in the three bulk sediment cores was 17 μM (Table 1). Porewater phosphate concentrations are much higher than phosphate concentrations in the water column. Kalnejais (2010) reported surface porewater concentrations of 70 μM taken in October from a core in Hingham Bay, Boston Harbor. The concentrations measured here are lower, likely because of reduced activity in the sediments over winter.

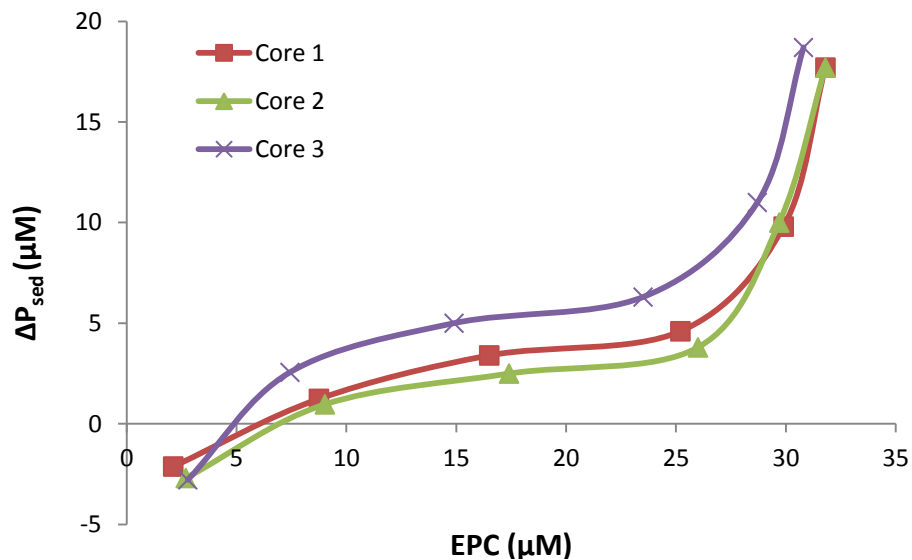


Figure 1: Adsorption isotherms as a function of EPC, or the final aqueous phosphate concentration for the bulk sediment samples. ΔP_{sed} represents the phosphate that was adsorbed onto the sediments from the water during the experiment. Cores 1, 2, and 3 were taken from the same location in Great Bay in triplicate. Uncertainty in the data points was determined from replicate incubations at a fixed added phosphate concentration. Uncertainty in core 1 was ± 0.15 in both the x- and y-directions. Error in core 2 was ± 0.01 in both the x- and y-directions. Error in core 3 was ± 0.3 in both the x- and y-directions.

Figure 1 above shows the adsorption isotherms from each of the three cores. EPC is the equilibrium phosphate concentration, or the final phosphate concentration in the seawater after 24 hours of shaking. The adsorption isotherms show how the amount of phosphate adsorbed to the sediments changes as the equilibrium phosphate concentration increases. All three isotherms show a leveling off at about 25 μM for EPC, followed by a steady, rapid increase in adsorption above 25 μM . Core 3 shows a slightly higher adsorption capacity than cores 1 and 2 and also a steeper initial adsorption from an EPC of 3 to 8 μM . This could be due to random variations in sedimentary phosphorus or mineralogy of the sediments collected even though all three cores were collected under the same conditions in the same location.

Great Bay sediment seems to behave differently than calcareous sediment from Florida Bay where the same experimental methods were used (Zhang & Huang, 2007). In Florida Bay, the adsorption isotherms decreased in slope as EPC increased and also appeared to approach a maximum ΔP_{sed} value. In the Great Bay sediments, the adsorption isotherms seem to approach a threshold EPC value where adsorption rates suddenly increase. The Florida Bay sediment maximum value can be explained by a reduction in spaces available for phosphate to adsorb onto the sediments. However, in the Great Bay sediments, there seems to be some kind of chemical reaction occurring in the sediments that allows for the availability of more adsorption sites once the threshold EPC value is approached.

On Figure 1, an EPC value of 17 μM appears to be the EPC at which there is the greatest amount of leveling off for all three isotherms. Considering the sediments are in contact with the porewater, it can be assumed that the porewater represents an equilibrium phosphate concentration in the estuarine environment (Zhang & Huang, 2007). It would therefore make sense that the least amount of change in adsorption or desorption with the sediments is going on

at 17 μM . However, when the concentration of phosphate in the system increases, the sediments have to readjust to a new environment. In order to reach equilibrium again, much more phosphate has to be adsorbed.

Simulation of Sediment Erosion

Figure 2 below shows the effect of shear stress on the amount of total suspended solids (TSS) in the water column of the erosion chamber. TSS remained at 0.0 until a shear stress of approximately 0.26 N/m^2 was reached. The threshold shear stress occurred when the imposed shear stress of the propeller exceeded the cohesive forces of the sediments (Kalnejais et al., 2007). The threshold shear stress was higher than anticipated, which may be due to polysaccharide formation from the visible algal mat on the surface of the sediments. Polysaccharides create a stronger than normal barrier that likely increase cohesive strength on the surface. When the threshold value of 0.26 N/m^2 was finally reached, the algal mat broke up and the underlying sediments began to erode. It is uncertain whether the algal mat had a significant effect on the phosphate adsorption experiments in terms of the amount of sediment that could be eroded from the erosion chamber. The effect of the algal mat on phosphate adsorption could be observed by collecting another sediment core, one without an algal mat, and repeating the procedure.

In a sediment resuspension experiment by Kalnejais et al. (2007) using the same erosion chamber, an algal mat also formed that may have decreased erodibility; the threshold values where a significant amount of sediment was resuspended were 0.11 N/m^2 in the fall and 0.14 N/m^2 in June. The reason for such a high threshold value in our experiment could be the

presence of a thicker algal mat, the variation with geographic location, or the seasonal variation considering this experiment took place in March after the first few sunny days in spring.

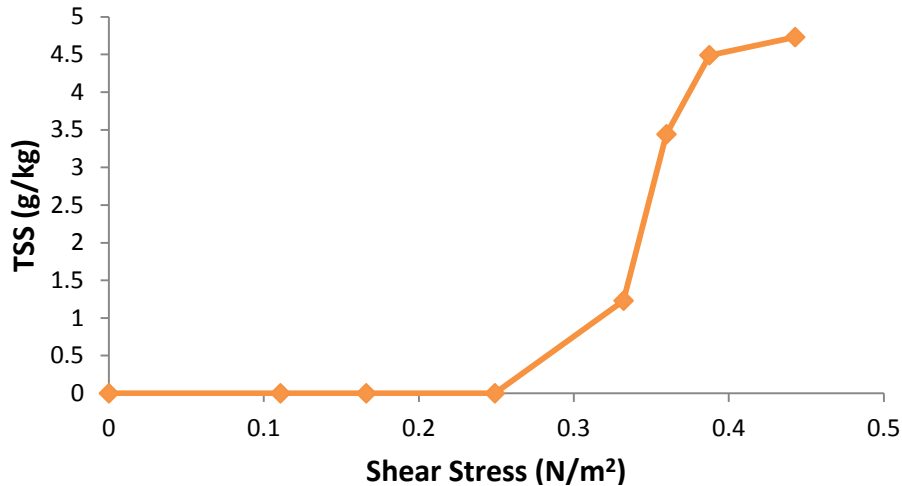


Figure 2: The effect of shear stress on the total suspended solids (TSS) found in the water column.

Table 2 below shows the depth eroded into the sediment core at each shear stress that was used in phosphate adsorption experiments. Erosion depth at shear stresses of 0.39 and 0.44 N/m² were, respectively, 5 mm and 5.3 mm. Compared to the 0.33 N/m² erosion depth of 1.4 mm, the other two erosion depths were very similar. This could explain the similarities in adsorption characteristics that are shown below in Table 3. It also explains why TSS data for these two shear stresses were likewise very similar (Figure 2).

Shear Stress (N/m ²)	Depth of Core Eroded (mm)
0.33	1.4
0.39	5.0
0.44	5.3

Table 2: The effect of shear stress on erosion depth of the sediment core. Known values for the calculation included the following: 1.7 L (water volume in chamber), 10.8 cm (core barrel diameter), 0.85 (sediment porosity), 2.65 g/cm³ (density of solids in sediment), 1.025 g/cm³ (density of sea water), and TSS data from Figure 2.

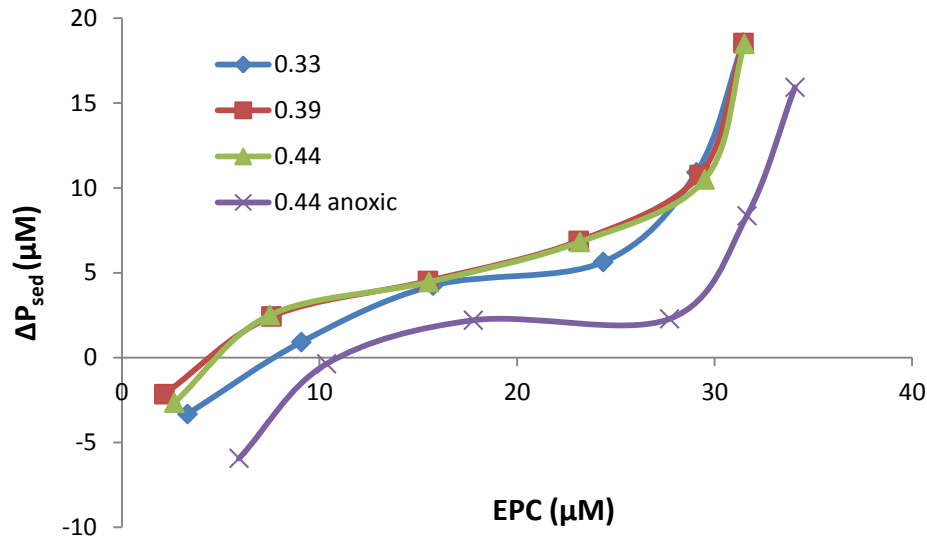


Figure 3: Adsorption isotherms as a function of EPC, or the final aqueous phosphate concentration for the erosion experiment samples. ΔP_{sed} represents the phosphate that was adsorbed onto the sediments from the water during the experiment. The 0.44 N/m^2 sample was divided in half, and one sample was run under nitrogen gas to remove the effect of oxygen redox chemistry on phosphate adsorption. Uncertainty determined by replicate experiments for the 0.33 N/m^2 sample was ± 0.6 in both the x- and y- directions. Error for the 0.39 N/m^2 sample was ± 0.9 (x) and ± 0.8 (y). Error for the 0.44 N/m^2 sample was ± 0.2 in both the x- and y-directions. Error for the 0.44 N/m^2 anoxic sample was ± 0.2 (x) and ± 0.3 (y).

In Figure 3 above, adsorption isotherms were determined for three different shear stresses: 0.33, 0.39, and 0.44 N/m^2 . All four samples showed the same pattern as the bulk sediment adsorption isotherms: a leveling off followed by a rapid, steady increase. The slope of the 0.33 isotherm leveled off at about 20 μM , but there was no distinct point of leveling off for the 0.39 and 0.44 isotherms. The isotherm under anoxic conditions seemed to level off at about 18 μM and then slightly decrease before rapidly increasing at about 28 μM . The lack of leveling off may suggest that different phases are responsible for phosphorus adsorption at higher shear stresses than in bulk sediment and early erosion samples.

Calculations

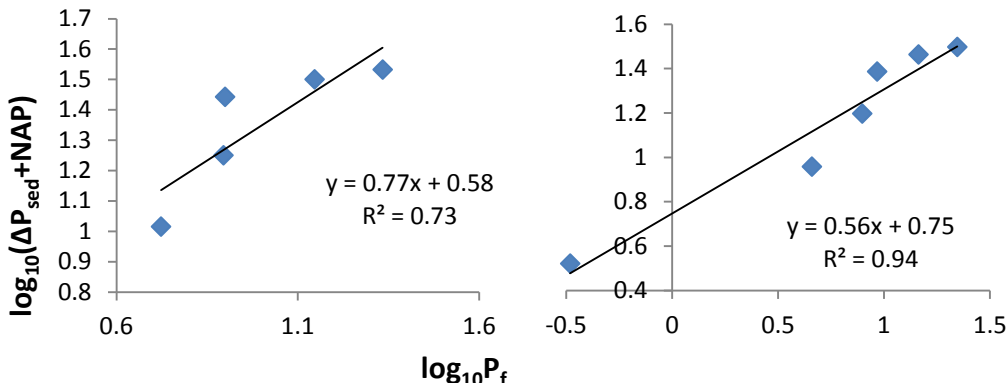


Figure 4: Example figures for how K_f and n were calculated from equation 3. K_f is equal to the slope of the linearization equation, and n is equal to the y-intercept of the linearization equation. These values were used to calculate K_d , the linear adsorption coefficient. Figure a) shows the lowest correlation with an r^2 of 0.73 and b) shows the highest correlation with an r^2 of 0.94.

Figure 4 above shows how phosphate adsorption was quantified from equation 3.

Equation 4 was used to calculate K_d , which is a linear adsorption coefficient. K_d is the equilibrium constant that describes the affinity of a solid for phosphate ions. The bigger the K_d for a given amount of solids, the more phosphate will be bound to the solid phase. The data in Figure 4 were linearized to obtain values needed for equation 4. The correlation coefficients of the linearization ranged from 0.73 to 0.94 (Table 3, Table 4). Equation 4 was derived from Zhang and Huang (2007), and it was assumed that the sediments from the Great Bay have the same adsorption characteristics. The lower r^2 values observed for some samples may suggest the sediments from this experiment behaved differently than the calcareous sediments of Florida Bay (Zhang & Huang, 2007), and the Freundlich adsorption model does not completely describe the sediment adsorption behavior. A possible future improvement to the accuracy of the results could be to remove the final two data points on each linearization plot in order to use data that more closely resemble the Freundlich model. In other words, recalculating K_d using only the first four data points may provide K_d values with higher correlation coefficients.

The adsorption capacity, as quantified by K_d values, was slightly lower at the 0.33 N/m² shear stress step compared to the 0.39 and 0.44 N/m² steps, indicating that as storm strength increases, the ability of resuspended sediments to adsorb phosphate also increases. Half of the sediment collected at a shear stress of 0.44 N/m² was used to observe the effect of redox chemistry on adsorption by performing the phosphate adsorption experiment under anoxic conditions. This sample showed weaker adsorption characteristics than all three other erosion samples. The anoxic conditions prohibited the oxidation of Fe(II) to form iron oxyhydroxides, which have a strong affinity to phosphate. The sediment eroded at higher shear stress having stronger adsorption is likely due to the release of dissolved Fe(II) from the sediments during erosion that is then oxidized in the water column to form strongly adsorbing iron oxyhydroxide particles.

The ability to adsorb was significantly less than the lowest shear stress sample (0.33 N/m²). The first material to be eroded has a lower K_d and therefore weaker phosphate adsorption than later material and also from bulk sediment (Table 3, Table 4). This could be because the very first material to be resuspended is recently settled organic matter that has not yet been incorporated into the sediments fully and that lacks strong P binding phases such as iron oxides. The bulk sediment and deeper eroded samples have higher iron content and phosphate adsorbs strongly to iron oxides (Lyons, 1982).

Core	NAP	n	K_d Avg	R^2
1	1.9	0.67	0.21 ± 0.08	0.78
2	2.5	0.63	0.19 ± 0.08	0.75
3	2.2	0.92	0.28 ± 0.02	0.81

Table 3: Results of calculations for the bulk sediment samples. NAP was calculated by linearizing the data from Figure 1. The calculation of n is shown in Figure 4. K_d was calculated using Equation 3. A K_d value was calculated for each sample, and then an average and standard deviation were calculated for each core. Six samples (each with a different $[P]_i$) were used for each core to calculate average and standard deviation.

Shear Stress (N/m ²)	NAP	n	K _d Avg	R ²
0.33	3.6	0.56	0.14 ± 0.06	0.94
0.39	1.9	0.91	0.29 ± 0.03	0.86
0.44	2.3	0.96	0.29 ± 0.01	0.83
0.44 anoxic	5.6	0.77	0.23 ± 0.04	0.73

Table 4: Results of calculations for the erosion experiment samples. NAP was calculated by linearizing the data from Figure 2. The calculation of n is shown in Figure 4. K_d was calculated using Equation 3. A K_d value was calculated for each sample, and then an average and standard deviation were calculated for each shear stress. Six samples (each with a different [P]_i) were used for each shear stress to calculate average and standard deviation.

The K_d value for the 0.44 N/m² anoxic sample was 0.06 lower than that of the oxic 0.44 N/m² sample. This supports the data from Figure 3 that suggest a decreased ability to adsorb phosphate when oxygen is not present to form iron oxides. However, the anoxic sample had a higher adsorption capacity than two out of three bulk samples and the erosion sample of the lowest shear stress (0.33N/m²). This suggests that the capacity to bind phosphate is still greater in eroded sediment from deeper within the sediment core. The K_d values for both the 0.39 and 0.44 N/m² samples were 0.29, suggesting that the samples had an equal ability to adsorb phosphate. It is possible that the sediment characteristics became more uniform with depth compared to surface sediments. Figure 2 also shows the difference in TSS between the two samples; it is much less than the difference between the two samples and every other shear stress sample. Therefore, erosion between 0.39 and 0.44 N/m² was very similar in adsorption behavior.

Data from this experiment fall within the K_d range found in Florida Bay by Zhang and Huang (2007): 0 – 0.6. K_d values in Florida Bay varied by geographic location and distance from land, often with the highest K_d values closest to the land and sources of phosphate such as river input. The range is so high because there were 40 sampling sites at the Florida Bay compared to a single sampling site in the Great Bay Estuary.

Future Work

Future work could examine the mineralogy of the sediments including P phases and iron content. Also, the effect of the algal mat could be better quantified, and another experiment could be conducted during the summer to examine seasonal effects on phosphate adsorption capacities. What is actually binding phosphorus in the surface sediments, and how can that binding potential be quantified? Is the release of phosphorus a possibility, and what are the implications of phosphorus release if so?

Conclusion

Sediment resuspension releases particles that strongly bind phosphate in the water column, so sediment resuspension may remove phosphate from the water and keep phosphate concentrations low in the Great Bay Estuary. The first material to be eroded binds phosphate weakly while sediments eroded from deeper in the sediment bind phosphate more strongly. Eroded sediments have a higher adsorption capacity than undisturbed bulk sediments from the sediment surface. The formation of iron oxides in the water column after erosion is likely to contribute to the higher K_d of eroded material. Finally, the K_d values found in the sediments of Great Bay fall within the values measured for other sediments, such as the sediments found in Florida Bay (Zhang & Huang, 2007).

References

- Diaz, R. & R. Rosenberg (2008). Spreading Dead Zones and Consequences for Marine Ecosystems. *Science* **321**: 926-929.
- Froelich, P. (1988). Kinetic control of dissolved phosphate in natural rivers and estuaries: A primer on the phosphate buffer mechanism. *Limnology and Oceanography*. **33**(4): 649-668.
- Joyce, S. (2000). The Dead Zones: Oxygen-Starved Coastal Waters. *Environ Health Perspect* **108**: a120-a125. <http://dx.doi.org/10.1289/ehp.108-a120>.
- Kalnejais, L. J., Martin, W. R. et al. (2007). The role of sediment resuspension in the remobilization of particulate-phase metals from coastal sediments. *Environmental Science & Technology* **41**: 2282-2288.
- Kalnejais, L. H., Martin, J. R., & M. H. Bothner. (2010). The release of dissolved nutrients and metals from coastal sediments due to resuspension. *Marine Chemistry* **121**: 224–235.
- Lyons (1982). Nutrient Porewater Chemistry, Great Bay, New Hampshire: Benthic Fluxes. *Estuaries* **5**(3): 230 – 233.
- PREP (2009). State of the Estuaries Report. Piscataqua Region Estuaries Partnership, University of New Hampshire, Durham, NH. Published online: www.prep.unh.edu/resources/pdf/2009_state_of_the-prep-09.pdf.
- Strickland, J. D. H. & T. R. Parsons (1977). *Practical Handbook of Seawater Analysis*, Fisheries Research Board.
- Warnken, K et al. (2000). Benthic Exchange of Nutrients in Galveston Bay. *Estuaries* **23**(5): 647-661.
- Zhang, J., Fischer, C., & P. Ortner (2004). Potential availability of sedimentary phosphorus to sediment resuspension in Florida Bay. *Global Biogeochemical Cycles* **18**: 1-14.
- Zhang, J, & X. Huang (2007). Relative importance of solid-phase phosphorus and iron on the sorption behavior of sediments. *Environ. Sci. Technol.* **41**: 2789-2795.

Appendix

Figure 1

Core 1	EPC	ΔP_{sed}	Core 2	EPC	ΔP_{sed}	Core 3	EPC	ΔP_{sed}
A	2.27	-2.27	A	2.69	-2.69	A	2.78	-2.78
A _{dup}	1.97	-1.97	B	9.03	0.96	B	7.43	2.56
B	8.75	1.24	B _{dup}	9.01	0.98	C	15.2	4.70
C	16.5	3.40	C	17.4	2.50	C _{dup}	14.6	5.30
D	25.6	4.20	D	26.0	3.80	D	23.5	6.30
D _{dup}	24.8	5.00	E	29.7	10.0	E	28.7	11.0
E	29.9	9.80	E _{dup}	29.7	10.0	F	30.8	18.7
F	31.8	17.7	F	31.8	17.7			

Figure 2

Shear Stress (N/m ²)	TSS (g/kg)
0	0.0
0.11	0.0
0.17	0.0
0.25	0.0
0.33	1.23
0.36	3.44
0.39	4.49
0.44	4.73

Figure 3

0.33 N/m ²	EPC	ΔP_{sed}	0.39 N/m ²	EPC	ΔP_{sed}	0.44 N/m ²	EPC	ΔP_{sed}
A	2.69	-2.69	A	2.15	-2.15	A	2.65	-2.65
A _{dup}	3.94	-3.94	B	7.57	2.43	B	7.49	2.51
B	9.08	0.92	C	14.6	5.35	C	15.5	4.46
C	15.7	4.25	C _{dup}	16.3	3.68	E	23.2	6.82
D	24.4	5.64	D	23.1	6.88	E	29.3	10.7
E	29.1	10.9	E	29.2	10.8	E _{dup}	29.7	10.3
F	31.4	18.6	F	31.5	18.5	F	31.5	18.5

(Figure 3 continued)

0.44 N/m² anoxic	EPC	ΔP_{sed}
A	5.93	-5.93
B	10.4	-0.36
C	17.8	2.21
D	27.5	2.50
D _{dup}	27.9	2.07
E	31.6	8.36
F	34.1	15.9